Analyst

PAPER

FTIR imaging detects diet and genotype-dependent chemical composition changes in wild type and mutant *C. elegans* strains†

Cite this: DOI: 10.1039/c7an01432e

A. Bouyanfif,[a,b,c] S. Liyanage,[a,c] J. E. Hewitt,[c,d] S. A. Vanapalli,[c,d] N. Moustaid-Moussa,[a,b,c] E. Hequet[a] and N. Abidi*[a,c]

Received 29th August 2017,
Accepted 8th November 2017

DOI: 10.1039/c7an01432e

rsc.li/analyst

This study focuses on the use of Fourier Transform Infrared (FTIR) microspectroscopy to determine chemical changes induced in the nematode *Caenorhabditis elegans* by supplementation of *C. elegans* maintenance media (CeMM) by Eicosapentaenoic acid (EPA). Wild-type *C. elegans* (N2) and mutant strains (*tub-1* and *fat-3*) were grown in CeMM alone, and CeMM supplemented with EPA at 25 or 100 μM. Feeding was performed for 72 h. FTIR imaging was performed in transmission mode on individual worms. The FTIR imaging analysis of wild-type animals revealed the presence of vibrations assigned to unsaturated fatty acids, specifically bands at 3008 cm^{-1} (=C–H, olefinic stretch) and 1744 cm^{-1} (C=O, unsaturated fatty acids). It confirmed previously reported synthesis of unsaturated fatty acids in wild-type *C. elegans*. For the FTIR spectra of mutant strains, these vibrations were absent or present only as very small shoulder, which indicates that *tub-1* and *fat-3* synthesize essentially saturated fatty acids as indicated by the presence of $-CH_2$ and C=O vibrations. These results are in agreement with previous studies which reported that these mutants have altered lipid compositions. Principal component analysis showed differences in chemical composition between wild-type and mutant strains as well as between mutant strains cultured in normal CeMM and those cultured in CeMM supplemented with EPA. This study demonstrated the usefulness of FTIR microspectroscopy to investigate fat metabolism in *C. elegans*.

Introduction

Obesity is a disease of multifactorial etiology.[1] Its pathogenesis is influenced by diet, physical activity, age, environmental, and genetic factors. Due to an imbalance between pro-inflammatory *vs.* anti-inflammatory signaling and free radical production *vs.* antioxidant factors produced, obesity is associated with chronic low-grade inflammation and oxidative stress. It has been reported that omega-3 polyunsaturated fatty acids (ω-3 PUFAs) reduce obesity-associated inflammation and dyslipidemia. When supplemented with diet, ω-3 PUFA eicosapentaenoic acid (EPA) prevented and reversed hepatic steatosis, glucose intolerance, insulin resistance, and reduced adipose and systemic markers of inflammation and oxidative stress in mice fed a high-fat diet.[2] Omega-3 fatty acids are also potent anti-inflammatory dietary compounds. Omega-3 fatty acids or n-3 fatty acids are a key family of polyunsaturated fatty acids with a double bond at the third carbon atom from the methyl moiety of the carbon chain.[3] Also known as essential fatty acids (EFAs), omega-3 fatty acids are needed by the body for a number of functions and are important for normal metabolism and good health. However, mammals, including humans, are unable to synthesize omega-3 fatty acids *de novo* because of the lack of endogenous enzymes delta-12 desaturase and delta-15 desaturase for ω-3 desaturation. Therefore, mammals must get these fatty acids from the diet.[4] Studies of effects of omega-3 fatty acids in mammals, especially in humans, present several challenges including difficulty to manipulate and/or control intake of these fatty acids from the diet. The nematode *Caenorhabditis elegans* is an excellent model for such studies, as the wild-type (WT) naturally makes these long chain fatty acids. Furthermore, various mutant strains lacking specific PUFA synthesis enzymes are already available. Moreover, due to easy culturing of this organism, varying amounts and types of PUFAs can be added to the diets and compared to the WT strain, which synthesizes very long chain PUFAs such as EPA.

[a]*Department of Plant and Soil Science, Fiber and Biopolymer Research Inst, USA. E-mail: noureddine.abidi@ttu.edu*
[b]*Department of Nutritional Sciences, USA*
[c]*Obesity Research Cluster, USA*
[d]*Department of Chemical Engineering, USA*

† Electronic supplementary information (ESI) available: Infrared vibration assignments and principal components as function of wavenumbers. See DOI: 10.1039/c7an01432e

The possibility of using *C. elegans* as a model organism for evaluating lipid metabolism, inflammation, and oxidative stress in obesity-related studies has created the need for analytical techniques that can be used to determine the chemical composition on small and intact samples.

Fourier Transform Infrared (FTIR) microspectroscopy is a non-destructive technique for the study of various materials including biological samples.[5–7] It provides information on the presence of chemical species as well as their distribution within a sample. The IR spectrum of a material is made of absorption peaks, which represent frequencies of vibrations between bonds of the molecules making up the material. Because different materials have a unique combination of molecules, they exhibit different IR signatures. Thus, the IR spectra provide a unique chemical fingerprint of the samples.

FTIR microspectroscopy imaging has been used previously as a tool to study *C. elegans* and their chemical composition.[8–11] The absorption of infrared radiation and its interaction with the vibrational modes of the atoms and chemical bonds led to useful information related to the chemical composition of the microorganism. Ami *et al.* reported on the use of FTIR microspectroscopy to study dried but intact *C. elegans* nematode.[9] It was the first reported FTIR investigation on a complex whole nematode. The use of the IR microscope allowed the authors to acquire IR spectra from different areas of a single worm: pharynx, intestine, and tail areas. It was reported that because of the difference in the FTIR spectra between the pharynx, intestinal, and tail regions, the absorption spectra from the pharyngeal areas could be used to distinguish between different nematode species. According to the authors, amide I and amide II protein bands, assigned to the vibrational modes of the backbone amine bonds, were of particular interest because, as reported previously, the stretching mode of the C=O is sensitive to the protein secondary structures.[12] The analysis of amide I indicated that different regions of the worms are composed of different proteins. Furthermore, it was concluded that collagen was the principal component of the tail.[9]

Recently, Sheng *et al.* reported on the use of FTIR microspectroscopy for the analysis of the biochemical composition of *C. elegans* worms.[11] The authors' justification for the use of this technique was that the traditional biochemical techniques for chemical composition analysis require relatively large amounts of materials. The authors demonstrated that FTIR could be used to detect changes in the relative levels of carbohydrates, proteins, and lipids on one single worm.[11] The IR results indicated that the relative intensities of the lipid-associated bands (2800–3000 cm^{-1}) were higher for the *daf-2* mutant intestines compared to those of the WT. The authors indicated that the results obtained from IR imaging are consistent with gas–liquid chromatography and that the *daf-2* mutant contains higher levels of triglycerides than WT. Furthermore, vibrations in the range 1140–1180 cm^{-1}, assigned to polysaccharides, showed high intensities in *daf-2* mutant compared to N2 WT.[11] The authors attributed this to the rate at which polysaccharides are synthesized from sugars or the rate at which polysaccharides are broken down.

FTIR was also used to investigate the role of trehalose sugar to preserve native membrane lipid packing during extreme desiccation followed by rehydration of dauer larva of *C. elegans*.[13] The results showed that desiccation and rehydration led to changes in the FTIR spectra. The authors concluded that the major effect of trehalose on membranes during desiccation is to preserve the native packing of lipids.[13]

These previous works using FTIR analysis on *C. elegans* have laid the foundation for further analyses on chemical composition of *C. elegans* under different conditions. In this work, we report on the use of FTIR microspectroscopy to investigate the chemical composition of wild-type (N2) *C. elegans* and mutant strains (*tub-1* and *fat-3*) when cultured in bacteria-free *C. elegans* maintenance media (CeMM) both without supplementation and supplemented with EPA at different concentrations. FTIR images were acquired in transmission mode on single worms. Through this work we have demonstrated that FTIR microspectroscopy can be used as a tool to study the effects of diets on the chemical composition of intact worms.

Experimental

Materials

Hermaphrodite adult WT(N2) and mutant strains, *tub-1* (*nr2044*) and *fat-3(wa22)*, were acquired from the *Caenorhabditis* Genetics Center (CGC, University of Minnesota, Minneapolis, MN, USA). Worms were initially cultured on NGM (nematode growth media) plates seeded with *E. coli* OP50 following standard protocols. Plates containing a large quantity of eggs and gravid adults were then bleached, and eggs were left overnight to hatch in sterile M9 Buffer. Starved L1 animals were then transferred the following day to CeMM (Cell Guidance Systems, Babraham, Cambridge, UK) containing 20 μg mL^{-1} kanamycin sulfate (Fisher Scientific) and 200 μg mL^{-1} streptomycin sulfate (Fisher Scientific), as reported previously.[14] All *C. elegans* strains were then cultured at 20 °C in axenic CeMM for multiple generations to allow the worms to adapt to the media before use in experiments.[15]

Eicosapentaenoic acid (EPA) was purchased from Nu-Check Prep (Elysian, MN, USA). It was supplied as omega-3 ethyl esters. The mass spectroscopy analysis showed that it was composed of 91.9% of EPA and 2.1% of DHA (docosahexanoic acid), and other fatty acids accounting for the remaining composition. Because EPA is sensitive to heat, light, and oxygen, care was taken to minimize exposure to these sources to prevent degradation by storing it at −80 °C. EPA solutions in ethanol with different concentrations were prepared. CeMM was supplemented with these EPA solutions at final concentrations of 25 and 100 μM, and feeding was performed for 72 hours on worm cultures of mixed ages.

FTIR microspectroscopy

C. elegans were washed with distilled water five times and individual Hermaphrodite adult worms were mounted on

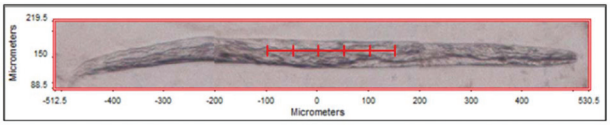

Fig. 1 Visual image showing the location form which spectra were acquired.

BaF_2 slides (PerkinElmer, MA, USA), which are transparent to IR radiation. Samples were then dried in a vacuum desiccator for 1 h. Images were collected using an FTIR microspectroscope equipped with a liquid nitrogen cooled 128 × 128 Mercury–Cadmium–Telluride (MCT) Focal Plane Array detector (Spotlight, PerkinElmer, MA, USA) in transmittance mode. One hundred twenty eight co-added spectra between 4000–1000 cm^{-1} were collected from each pixel (6.25 × 6.25 μm) with a spectral resolution of 16 cm^{-1} (8 cm^{-1} data point interval). The acquisition time of a typical image for a worm was around 3 h (worms were approximately 1000 μm long). A background spectrum, which is automatically subtracted from spectral data, was collected from an empty area of the slide. BaF_2 slides were systematically cleaned with water followed by acetone after collecting images.

In order to acquire a large number of spectra and perform principal component analysis, point mode FTIR microspectroscopy was used (line scans). In this case, the aperture size was set to 15 × 15 μm. Line scan images were collected from the middle part of worms along their length (8 worms from each treatment). The acquisition time of typical line scan images was around 20 min. Six to eight data points were acquired from each worm (separated by 50 μm) (Fig. 1). This generated between 48 and 64 FTIR spectra. It should be pointed out that the spectra extracted from images acquired using imaging mode are exactly similar to those acquired using point mode (data not shown). This indicates that using point mode to speed up image acquisition did not result in loss of information.

Spectroscopic data analysis

After acquiring IR images of the whole worms, individual spectra were extracted from the images of WT(N2), *tub-1*, and *fat-3* worms specifically from three different areas of the worms: head, middle, and tail. All spectra were baseline corrected and normalized using Spectrum 10™ software (PerkinElmer, MA, USA). Each infrared vibration in the spectra was assigned to a chemical functional group. Spectra were extracted also from each line scan images using the Spectrum Image software. The spectra were baseline corrected and normalized (with respect to the total absorbance over the entire range from 4000 to 650 cm^{-1}). Then principal component analysis was performed using Unscrambler® X 9.6 software (CAMO Software AS, Norway).

Results and discussion

Wild-type cultured in CeMM without supplementation

WT *C. elegans* were cultured in CeMM without supplementation and FTIR images were collected from the region of interest (ROI). The acquired IR spectra contain information on the chemical composition from the ROI, which in our case was either the head, middle, or tail region of the worms. Fig. 2a and b shows a visual image of a WT worm and the corresponding IR image acquired in transmission mode. The extracted IR spectra from the head, middle, and tail regions indicated by the squares on the IR map are shown in Fig. 2c. Table S1† summarizes the main vibrations along with their functional group assignments.

The FTIR spectra extracted from the head, middle, and tail regions of WT animals indicate differences in functional group distribution. The major differences are in the vibrations 3008 cm^{-1} (assigned to –CH═CH– stretching), 2928 and 2848 cm^{-1} (asymmetric and symmetric C–H stretching respectively), and 1744 cm^{-1} (C═O stretching). The integrated intensities of these vibrations were calculated (Fig. 3–5), and the integrated intensity of 3008 cm^{-1} is 340% higher in the middle region compared to the tail and head regions. This clearly indicates that unsaturated fatty acyl groups are present mainly in the middle region. Furthermore, the integrated

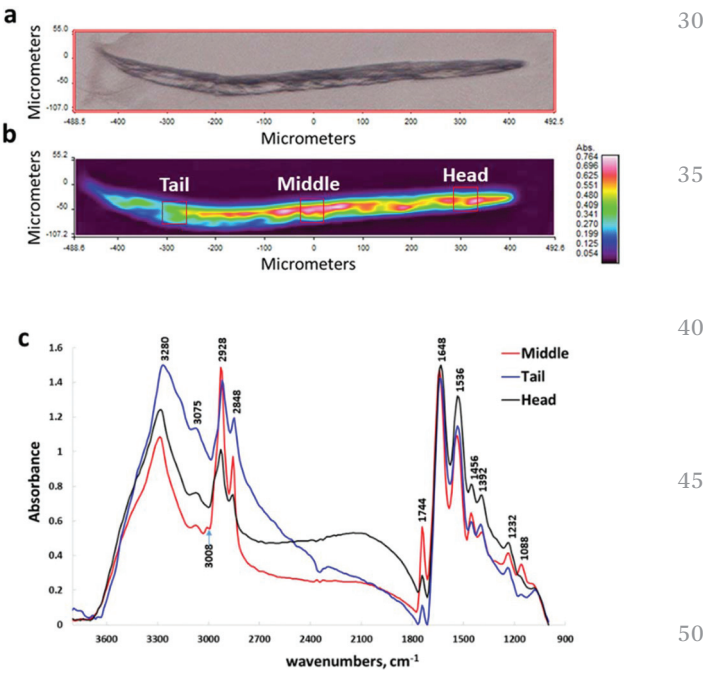

Fig. 2 FTIR detects differences in functional groups distribution in different regions of WT *C. elegans*: (a) visual image. (b) Corresponding IR image. The red color indicates higher concentration of functional groups while the purple color indicates low concentration. The distribution of colors indicates changes in the distribution of the chemical composition. (c) Extracted IR spectra from head, middle, and tail regions of WT *C. elegans* showing that FTIR can detect differences in chemical composition in different regions of the worm.

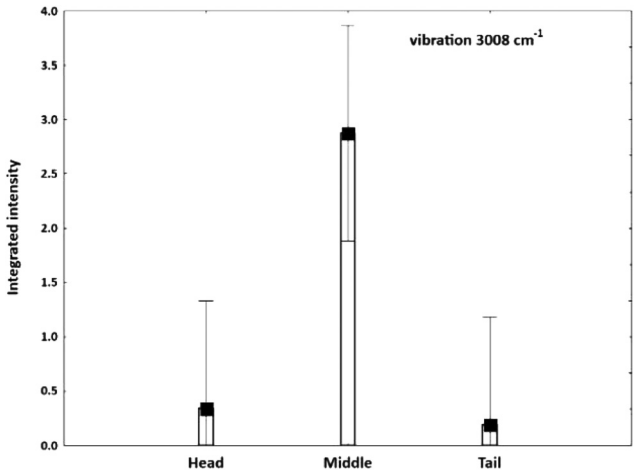

Fig. 3 Integrated intensity of the vibration 3008 cm^{-1} associated with unsaturated fatty acids present in the head, middle, and tail regions of WT(N2) (variance ratio (2, 9) = 11.883, p = 0.00298, vertical bars denote 0.95 confidence intervals).

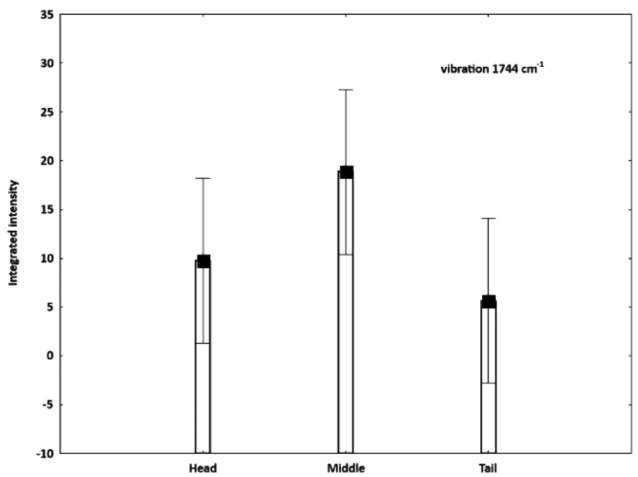

Fig. 4 Integrated intensity of the vibrations 2928 and 2855 cm^{-1} associated with lipids present in the head, middle, and tail regions of WT (N2) (variance ratio (2, 9) = 12.875, p = 0.00229, vertical bars denote 0.95 confidence intervals).

intensity of both 2928 and 2848 cm^{-1} is 136% higher and that of 1744 cm^{-1} is 218% higher in the middle region than in the head and tail regions. These results indicate that saturated acyl groups are stored mainly in the intestine regions along with unsaturated fatty acids. It has been reported that *C. elegans* stores fat mainly in droplets within the hypodermal and intestinal cells.[1,16] In these studies, fat storage in *C. elegans* has been quantified by measuring the intensity of staining by lipid-binding dyes (such as Nile Red, Oil Red O, and Sudan Black)[17,18] or by microscopy techniques such as Coherent Anti-Stokes Raman Scattering (CARS) and Stimulated Raman Scattering (SRS).[19,20]

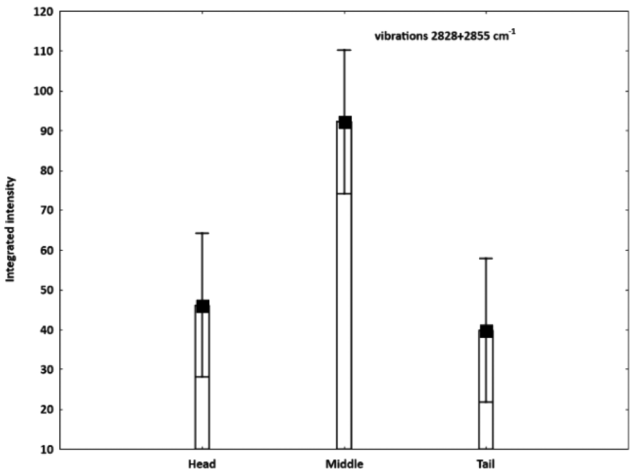

Fig. 5 Integrated intensity of the vibration 1744 cm^{-1} associated with fatty acids, triglycerides, phospholipids, or esters present in the head, middle, and tail regions of WT(N2) (variance ratio (2, 9) = 3.2760, p = 0.08532, vertical bars denote 0.95 confidence intervals).

WT, *tub-1*, and *fat-3* cultured in CeMM without supplementation

The above results confirmed previous studies which reported that the middle region is the main storage region for lipids and fats in wild-type animals. Because the objective of this study is to investigate the application of FTIR microspectroscopy to study fat storage in wild-type and mutant strains *C. elegans*, we focused on the middle part of the worm (which contains the intestines). We then proceeded with looking at the FTIR spectra of mutant strains *tub-1* and *fat-3* in addition to wild type (Fig. 6). Different vibrations are identified and their assignments are summarized in Table S1.†

Vibration 3280 cm^{-1}: This vibration, assigned to N–H stretching in amide A, originates from proteins.[21] The intensity of this vibration is high in mutant strains, which indicates that

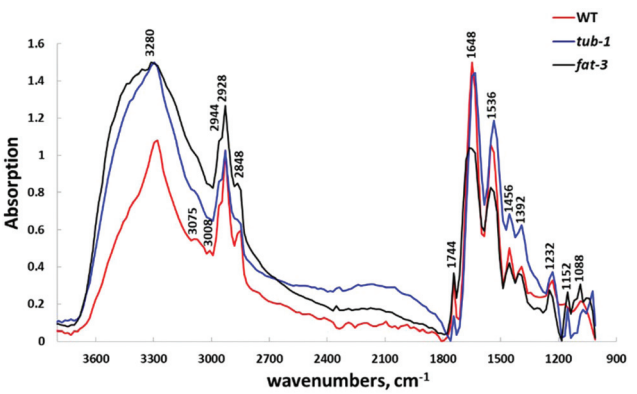

Fig. 6 FTIR spectra of WT, *tub-1*, and *fat-3 C. elegans* acquired from the middle region. Worms were cultured in CeMM without supplementation.

high ratio of proteins/fats is present in mutant strains compared to WT.

Vibration 3008 cm^{-1}: The presence in the spectra of WT of an additional vibration at 3008 cm^{-1} (which is assigned to =CH– stretch of olefin[21,22]) is very important to distinguish between WT and mutant strains *tub-1* and *fat-3*. This vibration originates from unsaturated fatty acids contained in the middle region of WT. This vibration is absent from the spectra of the mutant strains, indicating that mutant strains have lipid distribution different from those of wild type.

Vibrations 2928 and 2848 cm^{-1}: The C–H bonds absorb IR between 2800 and 3000 cm^{-1}. Two vibrations are noticed, 2928 cm^{-1} is assigned to asymmetric $-CH_2$ stretching while the vibration 2848 cm^{-1} is assigned to symmetric $-CH_2$ stretching.

Vibration 1744 cm^{-1}: The vibration 1744 cm^{-1} (C=O stretch) originates from fatty acids triglycerides, phospholipids, or cholesterol esters. The integrated intensity of this vibration was calculated from the spectra of the worms. The results show relatively higher triglycerides content in *fat-3* as compared to WT and *tub-1*.

Vibration 1648 cm^{-1}: This vibration (mainly from C=O stretching) is assigned to amide I in proteins (α-helix components of proteins).[23] It is interesting to notice that in *fat-3*, the intensity of this vibration is low compared to WT and *tub-1*. This could indicate that the relative amounts of all proteins is lower since there is more lipids *fat-3*.

Vibration 1536 cm^{-1}: This vibration originates from amide II (N–H bending and C–N stretching of proteins amide groups).[24] It was reported also that amino acid side chains (such as arginine, aspartate, glutamate, and tyrosine) or N–H groups from nucleotides could contribute to this vibration.[24] The intensity of this vibration is low in the case of *fat-3*.

Vibration 1456 cm^{-1}: This vibration, assigned to $-CH_2$ bending and deformation, could originate from lipids, proteins, or cholesterol esters.

Vibration 1392 cm^{-1}: This vibration is attributed to COO^- symmetric stretching and could originate from carbohydrates, fatty acids, and amino acid side chains.

Vibration 1232 cm^{-1}: This vibration is assigned to PO_2^- antisymmetric stretching of phospholipids, nucleic acids, or phosphorylated proteins.

Vibration 1152 cm^{-1}: This vibration is assigned to C–O stretching. It could originate from glycogen or mucin. It is interesting to notice that this vibration is only present as very small shoulder in the IR spectra of WT while it is an intense band in the spectra of mutant strains *tub-1* and *fat-3*.

Vibration 1088 cm^{-1}: This vibration is assigned to PO_2^- symmetric stretching of phosphodiesters. It could originate from nucleic acid (DNA and RNA), phospholipids, and glycolipids.

Several research groups have reported the biochemical composition of the fat content in *C. elegans*.[1,25–27] Column chromatography, thin-layer chromatography, and gas chromatography/mass spectroscopy were used in some of these studies. Ashrafi reported that triacylglyceride fats make up about 40 to 55% of total lipids,[28] and phospholipids are composed of about 55% ethanolamine glycerophospholipid, 32% choline glycerophospholipid, and 8% sphingomyelin.[1]

We collected several spectra from the middle of each worm and several worms from each strain. All spectra were normalized and baseline corrected according to the established procedure. Principal Component Analysis (PCA) was performed on the FTIR spectra in order to identify distinct groups of spectra.[29] This technique is widely used to reduce the dimensionality of the data from thousands of variables (wavenumbers) in the original spectra to a fewer number of dimensions. The variability in each spectrum relative to the mean of the population can be represented as a smaller set of values (axes) termed principal components (PCs). The effect of this process is to concentrate the sources of variability in the data into the first 2 or 3 PCs (PC-1, PC-2, and PC-3). Plots of PC-1 against PC-2 can reveal clustering in the FTIR spectra.

Fig. 7–9 shows the PCA of FTIR spectra of WT *vs. tub-1*, WT *vs. fat-3*, and *tub-1 vs. fat-3*. For WT *vs. tub-1*, PC-1 accounts for 76% of the variance, and it clearly separates the FTIR spectra into two groups: one for WT and one for *tub-1* (Fig. 7). A larger variability is noticed in the IR spectra of the *tub-1* mutant strain compared to WT. For WT *vs. fat-3*, PC-1 accounts for 81% of the variance, and it separates the FTIR spectra into two groups: one group of WT and one group of *fat-3* (Fig. 8). Again, a larger variability is noticed in the IR spectra of the *fat-3* mutant strain compared to WT. The discrimination between WT and the mutant strains indicates that differences in chemical composition between WT and mutant strains do exist. For *tub-1 vs. fat-3*, only few spectra of fat-3 can be separated from *tub-1*. Overall, IR spectra of *tub-1* are similar to those of *fat-3* (Fig. 9).

The discrimination between the IR spectra of WT and the mutant strains *tub-1* and *fat-3* may be due to differences in the chemical composition in the worm middle region. We attempted to interpret each PC scores in terms of differences in chemical composition. PC-1, PC-2, and PC-3 scores were plotted as function of wavenumbers (Fig. S1–S6, ESI†).

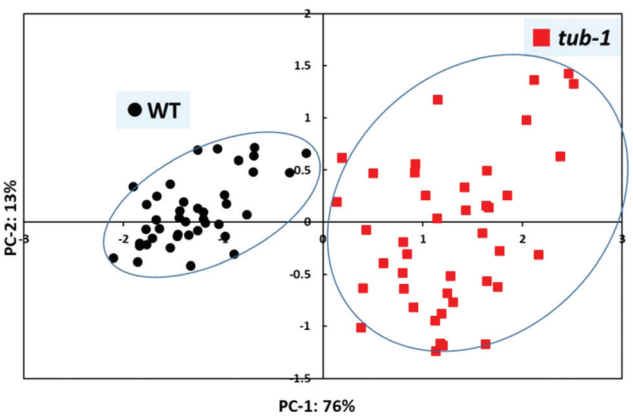

Fig. 7 Principal component analysis of FTIR spectra separates WT from mutant strain *tub-1*.

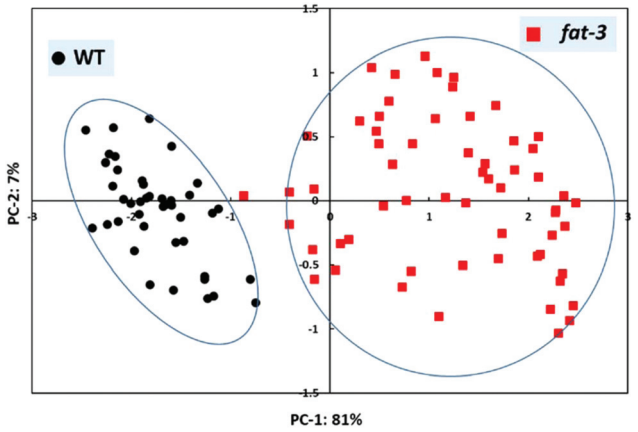

Fig. 8 Principal component analysis of FTIR spectra separates WT from mutant strain *fat-3*.

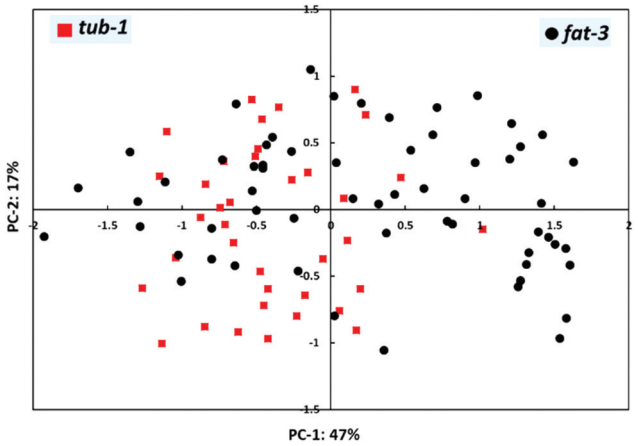

Fig. 9 Principal component analysis of FTIR spectra of mutant strains *tub-1 vs. fat-3*.

For *tub-1*, PC-1 scores presented in Fig. S1† show peaks at 3280, 2928, 1744, 1648, 1536, 1456, 1232, and 1152 cm^{-1}, which are characteristic of wavenumbers corresponding to proteins, lipids, phosphorylated lipids, and mucin (glycogen). PC-2 scores (Fig. S2†) show peaks at 2928, 2848, 1696, 1616, 1520 and 1392 cm^{-1}, which correspond to lipids and proteins. PC-3 scores (which explains 4% of variability) show also peaks characteristic of fatty acids (bands 3008, 2960, 2928, and 2884 cm^{-1}) and lipids (band 1744 cm^{-1}). A small peak is noticed at 3008 cm^{-1}, which corresponds to =CH– of unsaturated fatty acids. Other peaks are also noticed at 1664, 1472, 1392, 1232, and 1120 cm^{-1}.

For *fat-3*, PC-1 scores presented in Fig. S4† show peaks at 3280 cm^{-1} (vibration assigned to proteins), 3008 cm^{-1} (vibration assigned to unsaturated fatty acids), 2928 and 2855 cm^{-1} (vibrations assigned to lipids), 1744 cm^{-1} (vibration assigned to triglycerides, phospholipids, and fatty acids), 1648 cm^{-1} and 1536 cm^{-1} (vibrations assigned to proteins), and 1456 cm^{-1} (vibration assigned to lipids and proteins).

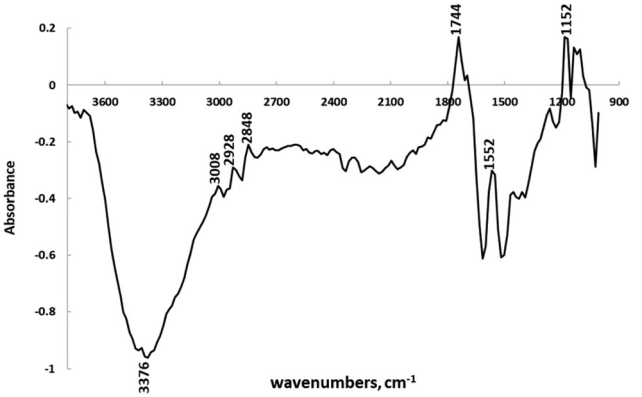

Fig. 10 Difference spectrum obtained by digital subtraction of *tub-1* spectrum from the WT spectrum.

PC-2 scores show also peaks at vibrations characteristic of lipids and proteins (Fig. S5†). PC-3 scores show important peaks at characteristic vibrations of unsaturated fatty acids and lipids (Fig. S6†).

To obtain additional information on the spectral differences between WT and mutant strains, we performed digital subtraction of the mutant strains spectra from WT spectra (Fig. 10 and 11). The major vibrations in the difference spectra are attributed to unsaturated fatty acids, lipids, and proteins (bands 3008, 2928, 2848, 1744, and 1648 cm^{-1}). It is worth pointing out that the intensity of the vibration 3008 cm^{-1} is high in the difference spectrum between WT and *tub-1*, while it is only a very small shoulder in the difference spectrum between WT and *fat-3*. Furthermore, the vibration 1648 cm^{-1} exists only as small shoulder in the difference spectrum between WT and *tub-1* while it is a sharp band in the difference spectrum between WT and *fat-3*.

The above IR results in Fig. 10 and 11 indicate that the major difference between WT and mutant strains *tub-1* (Fig. 10) and *fat-3* (Fig. 11) are unsaturated and saturated lipids. Previous research reported that WT *C. elegans* can syn-

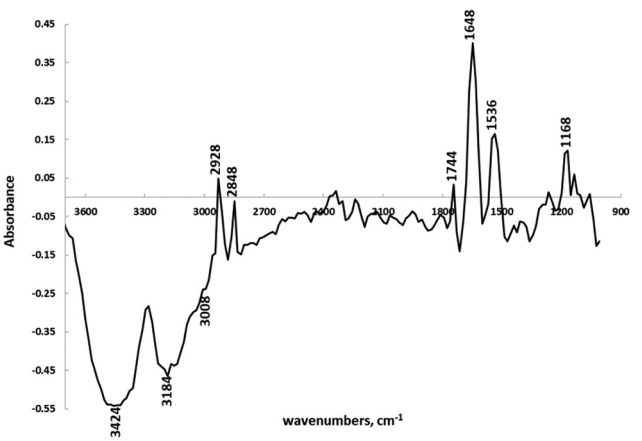

Fig. 11 Difference spectrum obtained by digital subtraction of *fat-3* spectrum from the WT spectrum.

thesize a wide range of saturated, monosaturated, and polysaturated fatty acids (including arachidonic acid (20:4n-6), eicosapentaenoic acid (20:5n-3), and monoethyl branched chain fatty acids).[25,26,27,29,30] However, the mutant strain *tub-1* is reported to exhibit increased fat accumulation,[1] while *fat-3* mutants were reported to lack Δ6 fatty acids and are deficient in C20 fatty acids (fatty acids C20:4n6, C20:4n3, and C20:5n3 are not detectable but high levels of 18:1n7, 18:2n6, and C8:3n3 are present).[27]

Worms cultured in CeMM supplemented with EPA

CeMM was supplemented with different concentrations of EPA (25 or 100 μM). FTIR was performed as described above. The objective was to investigate the chemical changes and relative levels of carbohydrates, proteins, and lipids induced by supplementing the growth media with unsaturated fatty acids using FTIR microspectroscopy. We believe that FTIR can be a valuable tool to add to the current techniques used for metabolic research of *C. elegans*. The FTIR spectra were collected from several individuals (8 worms and 6 to 8 spectra from each worm) from the middle region of the worms. All spectra were normalized and baseline corrected. It was followed by principal component analysis.

Wild type (N2): Fig. 12 shows the PCA of the spectra of WT cultured in CeMM without supplementation and WT cultured in media supplemented with EPA at 25 or 100 μM. PC-1 accounts for 57% of the variance and clearly separates the FTIR spectra into two groups: one group for WT and one group for WT when cultured in media supplemented with fatty acids. PC-2 accounts for 22% of the variance and PC-3 for 6% (data not shown). A larger variability is observed in the IR spectra of WT cultured in the fatty acids supplemented media. The separation of IR spectra into two distinct groups indicates that supplementing the media with fatty acids induced biochemical changes. Although we discriminate between WT cultured in CeMM without supplementation and WT cultured in media supplemented with EPA, there is no difference between

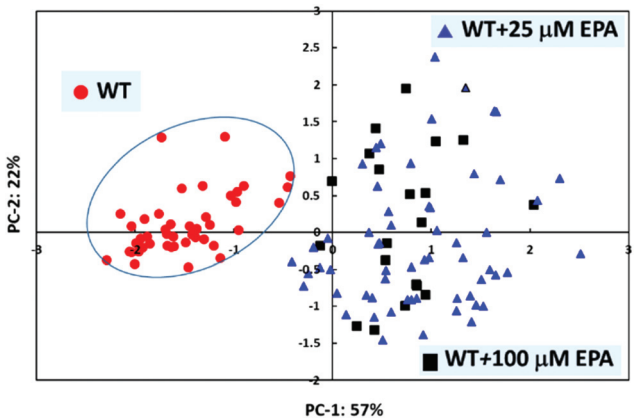

Fig. 12 Principal component analysis of FTIR spectra: WT cultured in CeMM without supplementation *vs.* WT cultured in CeMM supplemented with 25 or 100 μM of EPA.

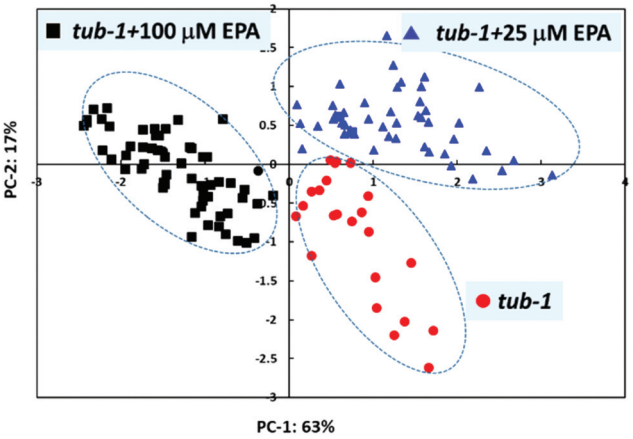

Fig. 13 Principal component analysis of FTIR spectra: *tub-1* cultured in CeMM without supplementation *vs.* *tub-1* cultured in CeMM supplemented with 25 or 100 μM of EPA.

supplementing with 25 or 100 μM. PC-1, PC-2 and PC-3 scores as function of wavenumbers (Fig. S7–S12†) show peaks at vibrations corresponding to lipids and proteins.

Mutant strain *tub-1*: Fig. 13 shows the PCA of FTIR spectra of the mutant strain *tub-1* cultured in CeMM without supplementation and in CeMM supplemented with 25 or 100 μM of EPA. PC-1 accounts for 63%, PC-2 accounts for 17%, and PC-3 accounts for 6% of the variance (data not shown). The FTIR spectra are clearly separated into three groups: one group for *tub-1* cultured in CeMM without supplementation, one group for *tub-1* cultured in CeMM supplemented with fatty acids at 25 μM, and one group for *tub-1* cultured in CeMM supplemented with 100 μM of EPA. It is of interest to note that both PC-1 and PC-2 are needed to separate the treatments into three groups (PC-1, PC-2 and PC-3 scores as function of wavenumbers are shown in Fig. S13–S15†).

Fig. 14 shows the PCA of the FTIR spectra of WT cultured in CeMM without supplementation and the mutant strain *tub-1* cultured in CeMM supplemented with 25 or 100 μM EPA. PC-1

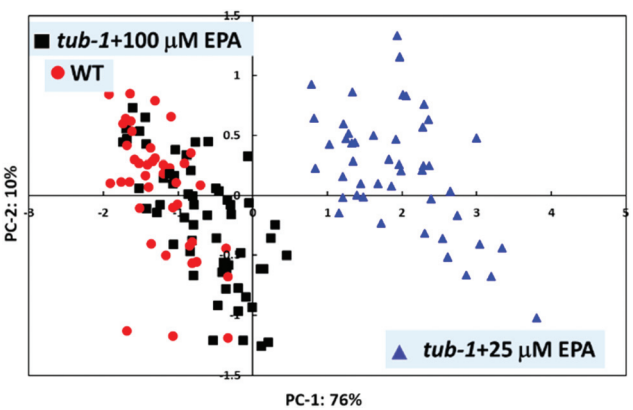

Fig. 14 Principal component analysis of FTIR spectra: WT cultured in CeMM without supplementation *vs.* *tub-1* cultured in CeMM supplemented with 25 or 100 μM of EPA.

accounts for 76% of the variance and separates the FTIR spectra into two groups: one group of spectra for *tub-1* cultured in CeMM supplemented with 25 μM of EPA and the second group is composed of the spectra of WT cultured in CeMM (no supplementation) and *tub-1* cultured in CeMM supplemented with 100 μM of EPA. It is interesting to notice that the spectra of *tub-1* with 100 μM are similar to the spectra of WT. These results indicate that supplementing the media with 100 μM of PUFAs makes the mutant strains *tub-1* (which lack the fatty acid synthase gene) behave as the wild type (which is able to make PUFAs). PC-1, PC-2 and PC-3 scores as function of wavenumbers are shown in Fig. S16–S18.†

Mutant strain *fat-3*: Fig. 15 shows the PCA of the FTIR spectra of *fat-3* cultured in CeMM with and without EPA supplementation. The spectra of *fat-3* cultured in CeMM supplemented with 25 or 100 μM EPA can be separated from those of the same mutant strain cultured in CeMM without supplementation. There is no separation in the spectra when supplementing with 25 or 100 μM (PC-1, PC-2 and PC-3 scores as function of wavenumbers are shown in Fig. S19–S21†).

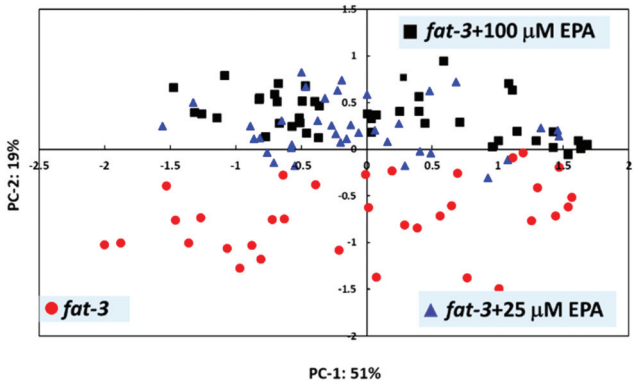

Fig. 15 Principal component analysis of FTIR spectra: *fat-3* cultured in CeMM without supplementation *vs.* *fat-3* cultured in CeMM supplemented with 25 or 100 μM of EPA.

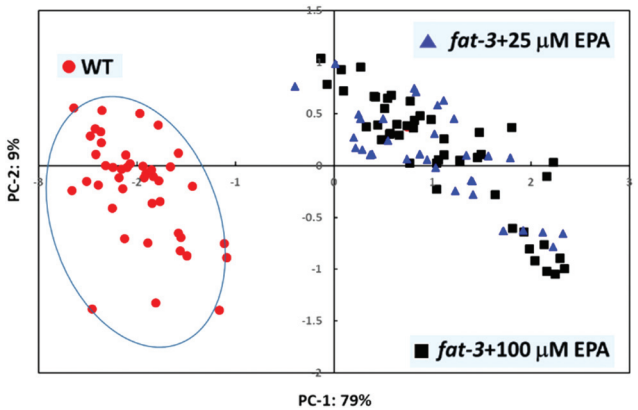

Fig. 16 Principal component analysis of FTIR spectra: WT cultured in CeMM without supplementation *vs.* *fat-3* cultured in CeMM supplemented with 25 or 100 μM of EPA.

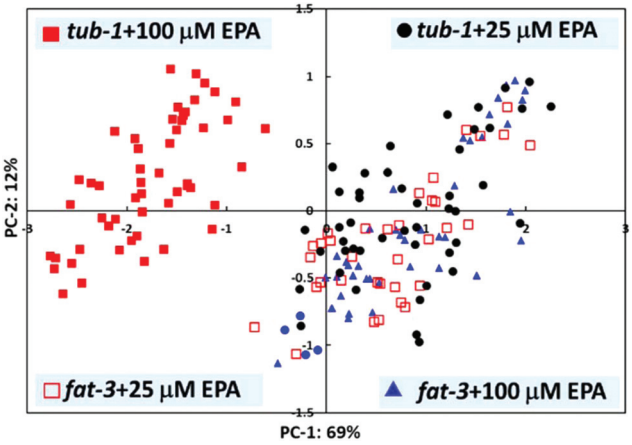

Fig. 17 Principal component analysis of FTIR spectra of mutant strains *tub-1* and *fat-3* cultured in CeMM supplemented with 25 or 100 μM of EPA.

Fig. 16 shows the PCA spectra of WT cultured in CeMM without supplementation and the mutant strain *fat-3* cultured in CeMM supplemented with 25 or 100 μM. PC-1 accounts for 79% of the variance and separates the spectra of WT from the spectra of *fat-3* cultured in CeMM supplemented with EPA (PC-1, PC-2 and PC-3 scores as function of wavenumbers are shown in Fig. S22–S24†). We can observe that supplementing the media with 25 or 100 μM leads to similar spectra. We can discriminate between WT and the mutant strain *fat-3* but not between the mutant strain subjected to different feedings. Contrary to the results obtained on *tub-1*, it appears that supplementing the media with 100 μM of PUFAs does not make the mutant strain *fat-3* behave as the WT.

As shown in Fig. 17, the PCA of the FTIR spectra of mutant strains *tub-1* and *fat-3* cultured in CeMM supplemented with 25 μM or 100 μM indicates that PC-1 (69% of the variance) separates the IR spectra of *tub-1* cultured in CeMM supplemented with 100 μM EPA from *tub-1* cultured in media supplemented with 25 μM and *fat-3* animals cultured in media supplemented with 25 μM or 100 μM EPA. PC-1, PC-2 and PC-3 scores as function of wavenumbers are shown in Fig. S25–S27.†

Conclusions

The FTIR microspectroscopy imaging analysis of WT revealed the presence of vibrations assigned to unsaturated fatty acids specifically the bands at 3008 cm^{-1} (assigned to =C–H from olefinic stretch) and 1744 cm^{-1} (assigned C=O from unsaturated fatty acids). This confirmed previous studies which reported the presence of unsaturated fatty acids in the wild-type of *C. elegans*. However, the IR spectra of the mutant strains (*tub-1* and *fat-3*) did not show the presence of the vibration 3008 cm^{-1} or it appeared as only a small shoulder. The major contribution came from saturated fatty acids as indicated by the -CH_2 and C=O vibrations. This confirmed that *tub-1* and *fat-3* do not synthesize considerable amount of

PUFAs. Principal component analysis clearly discriminated between wild-type and mutant strains cultured in CeMM with or without supplementation with EPA. PC-1, PC-2, and PC-3 scores as a function of wavenumbers showed peaks that are characteristics of unsaturated fatty acids, lipids, and proteins. Furthermore, digital subtraction of mutant strains spectra from WT spectra showed that the major vibrations in the difference spectra are attributed to unsaturated fatty acids, lipids, and proteins (bands 3008, 2928, 2848, 1744, and 1648 cm^{-1}). This study further demonstrates the usefulness of Fourier Transform Infrared microspectroscopy to study differences in chemical composition between wild-type and mutant *C. elegans* strains as well as to investigate fat metabolism and the impact of fatty acids when used as supplement in worms feeding media. The results obtained could be complemented by other studies such as targeted gene expression and biochemical analyses.

Conflicts of interest

There are no conflicts to declare.

Acknowledgements

Some strains used in this study were provided by the *Caenorhabditis* Genetics Center (CGC), which is funded by the NIH Office of Research Infrastructure Programs (P40 OD010440). The research was supported in part by NASA Grant # NNX15AL16G (SV), USDA NIFA AFRI #2015-67030-23452 (NMM, SV), the Obesity Research Cluster (NA, NMM), Texas Tech Transdisciplinary Research Academy (NMM, SV), and the Fiber and Biopolymer Research Institute (NA, EH).

References

1 K. Ashrafi, Obesity and the regulation of fat metabolism, *WormBook*, 2007, 1–20.
2 N. S. Kalupahana, K. Claycombe, S. J. Newman, T. Stewart, N. Siriwardhana, N. Matthan, A. H. Lichtenstein and N. Moustaid-Moussa, Eicosapentaenoic acid prevents and reverses insulin resistance in high-fat diet-induced obese mice via modulation of adipose tissue inflammation, *J. Nutr.*, 2010, **140**(11), 1915–1922.
3 J. L. Watts, Using Caenorhabditis elegans to Uncover Conserved Functions of Omega-3 and Omega-6 Fatty Acids, *J. Clin. Med.*, 2016, **5**(2).
4 A. P. Simopoulos, Genetic variants in the metabolism of omega-6 and omega-3 fatty acids: their role in the determination of nutritional requirements and chronic disease risk, *Exp. Biol. Med.*, 2010, **235**(7), 785–795.
5 M. J. Baker, J. Trevisan, P. Bassan, R. Bhargava, H. J. Butler, K. M. Dorling, P. R. Fielden, S. W. Fogarty, N. J. Fullwood, K. A. Heys, C. Hughes, P. Lasch, P. L. Martin-Hirsch, B. Obinaju, G. D. Sockalingum, J. Sule-Suso, R. J. Strong, M. J. Walsh, B. R. Wood, P. Gardner and F. L. Martin, Using Fourier transform IR spectroscopy to analyze biological materials, *Nat. Protoc.*, 2014, **9**(8), 1771–1791.
6 K. M. Dorling and M. J. Baker, Rapid FTIR chemical imaging: highlighting FPA detectors, *Trends Biotechnol.*, 2013, **31**(8), 437–438.
7 L. M. Miller, M. W. Bourassa and R. J. Smith, FTIR spectroscopic imaging of protein aggregation in living cells, *Biochim. Biophys. Acta*, 2013, **1828**(10), 2339–2346.
8 D. Ami, A. Natalello and S. M. Doglia, Fourier transform infrared microspectroscopy of complex biological systems: from intact cells to whole organisms, *Methods Mol. Biol.*, 2012, **895**, 85–100.
9 D. Ami, A. Natalello, A. Zullini and S. M. Doglia, Fourier transform infrared micro spectroscopy as a new tool for nematode studies, *FEBS Lett.*, 2004, **576**(3), 297–300.
10 L. Diomede, G. Cassata, F. Fiordaliso, M. Salio, D. Ami, A. Natalello, S. M. Doglia, A. De Luigi and M. Salmona, Tetracycline and its analogues protect Caenorhabditis elegans from beta amyloid-induced toxicity by targeting oligomers, *Neurobiol. Dis.*, 2010, **40**(2), 424–431.
11 M. Sheng, A. Gorzsas and S. Tuck, Fourier transform infrared microspectroscopy for the analysis of the biochemical composition of C. elegans worms, *Worm*, 2016, **5**(1), e1132978.
12 L. K. Tamm and S. A. Tatulian, Infrared spectroscopy of proteins and peptides in lipid bilayers, *Q. Rev. Biophys.*, 1997, **30**(4), 365–429.
13 C. Erkut, S. Penkov, H. Khesbak, D. Vorkel, J. M. Verbavatz, K. Fahmy and T. V. Kurzchalia, Trehalose Renders the Dauer Larva of Caenorhabditis elegans Resistant to Extreme Desiccation, *Curr. Biol.*, 2011, **21**(15), 1331–1336.
14 N. J. Szewczyk, I. A. Udranszky, E. Kozak, J. Sunga, S. K. Kim, L. A. Jacobson and C. A. Conley, Delayed development and lifespan extension as features of metabolic lifestyle alteration in C-elegans under dietary restriction, *J. Exp. Biol.*, 2006, **209**(20), 4129–4139.
15 N. J. Szewczyk, E. Kozak and C. A. Conley, Chemically defined medium and Caenorhabditis elegans, *BMC Biotechnol.*, 2003, **3**.
16 E. J. O'Rourke, A. A. Soukas, C. E. Carr and G. Ruvkun, C. elegans Major Fats Are Stored in Vesicles Distinct from Lysosome-Related Organelles, *Cell Metab.*, 2009, **10**(5), 430–435.
17 K. Ashrafi, F. Y. Chang, J. L. Watts, A. G. Fraser, R. S. Kamath, J. Ahringer and G. Ruvkun, Genome-wide RNAi analysis of Caenorhabditis elegans fat regulatory genes, *Nature*, 2003, **421**(6920), 268–272.
18 K. Yen, T. T. Le, A. Bansal, D. Narasimhan, J. X. Cheng and H. A. Tissenbaum, A Comparative Study of Fat Storage Quantitation in Nematode Caenorhabditis elegans Using Label and Label-Free Methods, *PLoS One*, 2010, **5**(9).
19 J. Zheng and F. L. Greenway, Caenorhabditis elegans as a model for obesity research, *Int. J. Obes.*, 2012, **36**(2), 186–194.

20 A. Folick, W. Min and M. C. Wang, Label-free imaging of lipid dynamics using Coherent Anti-stokes Raman Scattering (CARS) and Stimulated Raman Scattering (SRS) microscopy, *Curr. Opin. Genet. Dev.*, 2011, **21**(5), 585–590.
21 E. San-Blas, M. Guerra, E. Portillo, I. Esteves, N. Cubillan and Y. Alvarado, ATR/FTIR characterization of Steinernema glaseri and Heterorhabditis indica, *Vib. Spectrosc.*, 2011, **57**(2), 220–228.
22 H. Y. N. Holman, K. A. Bjornstad, M. C. Martin, W. R. Mckinney, E. A. Blakely and F. G. Blankenberg, Mid-infrared reflectivity of experimental atheromas, *J. Biomed. Opt.*, 2008, **13**(3).
23 A. Barth, Infrared spectroscopy of proteins, *Biochim. Biophys. Acta, Bioenerg.*, 2007, **1767**(9), 1073–1101.
24 A. J. Hobro and B. Lendl, Fourier-transform mid-infrared FPA imaging of a complex multicellular nematode, *Vib. Spectrosc.*, 2011, **57**(2), 213–219.
25 M. Kniazeva, M. Sieber, S. McCauley, K. Zhang, J. L. Watts and M. Han, Suppression of the ELO-2 FA elongation activity results in alterations of the fatty acid composition and multiple physiological defects, including abnormal ultradian rhythms, in Caenorhabditis elegans, *Genetics*, 2003, **163**(1), 159–169.
26 K. Satouchi, K. Hirano, M. Sakaguchi, H. Takehara and F. Matsuura, Phospholipids from the Free-Living Nematode Caenorhabditis-Elegans, *Lipids*, 1993, **28**(9), 837–840.
27 J. L. Watts and J. Browse, Genetic dissection of polyunsaturated fatty acid synthesis in Caenorhabditis elegans, *Proc. Natl. Acad. Sci. U. S. A.*, 2002, **99**(9), 5854–5859.
28 K. Ashrafi, Mapping out starvation responses, *Cell Metab.*, 2006, **3**(4), 235–236.
29 N. Abidi, L. Cabrales and C. H. Haigler, Changes in the cell wall and cellulose content of developing cotton fibers investigated by FTIR spectroscopy, *Carbohydr. Polym.*, 2014, **100**, 9–16.
30 M. Kniazeva, Q. T. Crawford, M. Seiber, C. Y. Wang and M. Han, Monomethyl branched-chain fatty acids play an essential role in Caenorhabditis elegans development, *PLos Biol.*, 2004, **2**(9), 1446–1459.